

Coupled-cluster pairing models for radicals with strong correlations

Susi Lehtola ^{1,2} and Martin Head-Gordon ^{1,3}

¹*Chemical Sciences Division, Lawrence Berkeley National Laboratory, Berkeley, California 94720, United States*

²*Department of Chemistry, University of Helsinki, P.O. Box 55 (A. I. Virtasen aukio 1), FI-00014 University of Helsinki, Finland^a)*

³*Department of Chemistry, University of California, Berkeley, California 94720, United States^b)*

The pairing hierarchy of perfect pairing (PP), perfect quadruples (PQ) and perfect hexuples (PH) are sparsified coupled-cluster models that are exact in a pairing active space for 2, 4, and 6 electron clusters, respectively. We describe and implement three extensions for radicals. First is the trivial generalization that does not correlate radical orbitals. The second model (PQr, PHr) includes terms that entangle pair indices and radical indices such that their maximum total number is 2 for PQ and 3 for PH (like their closed-shell versions). The third family of extended radical models (PPxr, PQxr, and PHxr) include cluster amplitudes that entangle up to 1, 2, and 3 pair indices with up to 1, 2, and 3 radical indices. Notably, PPxr and PQxr are exact for (3e,3o) and (5e,5o), respectively, while still having only $O(N)$ and $O(N^2)$ amplitudes like their parent models (for N paired electrons). Orbital optimization is considered for PPxr. A series of large-scale numerical tests of these models are presented for spin gaps, and ionization energies of polyenes and polyenyl radicals, ranging in size from ethene and allyl radical up to $C_{22}H_{24}$ in full-valence active spaces up to (122e,122o). The xR models perform best.

I. INTRODUCTION

Density functional theory^{1,2} (DFT) is by far the predominant framework for molecular electronic structure calculations, because it is computationally inexpensive, and because it is also sufficiently accurate for most applications.^{3,4} However, although DFT is formally exact for any system,^{1,2} in practice the deficiencies in density functional approximations to the exchange-correlation energy make DFT unreliable for systems where many configurations are important in the wave function.³ Similarly, normal single-reference wave function methods, such as low-order perturbation theory like second-order Møller–Plesset⁵ perturbation theory (MP2), or coupled-cluster (CC) theory with perturbative triples⁶ also do not adequately describe multi-configurational problems. As these problems arise frequently in several areas of chemistry, ranging from biradicaloids^{7,8} to polyradicaloid species such as multi-metal enzymes⁹ and related inorganic molecules with multiple (or even just one) spin centers,¹⁰ the treatment of strong correlation is a substantial challenge for electronic structure theory.

It is beyond reasonable limits to fully review all the activity and excitement that surrounds the strong correlation problem in chemistry today. However, for our purposes, it is useful to distinguish two broad approaches to avoiding the exponential cost of the exact solution of the Schrödinger equation. The first class of strong correlation methods are those that aim for the exact solution to within some, hopefully acceptable numerical tolerance. Conceptually, the simplest example of this class are the selected configuration interaction (CI) methods^{11–23} that attempt to identify the most important configurations while discarding the vastly larger set of so-called “configurational dead-wood”.^{24–26} Selected CI methods are closely related to the full CI quantum Monte-Carlo (FCI-QMC) approach,^{27–52} and are themselves now efficient enough to handle large systems,^{53–57} albeit still with soft exponential scaling. Many-body expansions of the exact energy offer yet another avenue to approach the full CI energy,^{58,59} as recently reviewed by Eriksen and Gauss⁶⁰. Another alternative is the density matrix renormalization group (DMRG) approach^{61–68} and emerging generalizations thereof,⁶⁹ which exploit low-rank wave function separability in a size-extensive way.

A second class of strong correlation methods make model wave functions that are compact relative either to full CI or to the above approximations. These methods aim to only capture the most significant correlations instead of all correlations within a numerical tolerance as in the first class of approaches. In other words, the methods in the second class seek a minimal reference wave function for strongly correlated systems to replace the Hartree–Fock (HF) method of single-reference theory. We note here that like HF, these methods omit dynamical correlation, and since dynamical correlation is necessary to attain quantitative accuracy, in general the methods have to be corrected in order to become reliable for chemistry; however, in this work we will focus exclusively on static correlation.

^a)Electronic mail: susi.lehtola@alumni.helsinki.fi

^b)Electronic mail: mhg@cchem.berkeley.edu

Because the strongest correlations are related to the low-energy one-particle excitations near the Fermi level, the model wave function approaches discussed above thus try to solve the Schrödinger equation only in the valence space, via well-defined models. This straight-away yields complete active space (CAS) methods,^{70,71} which solve the Schrödinger equation for some number of active electrons distributed into some number of active orbitals. As the dimension of the CAS problem is smaller than that of the untruncated Schrödinger equation, approximations such as selected CI,^{72–74} and DMRG^{75–77} can be applied to the CAS problem more effectively than to the untruncated Schrödinger equation.

As originally suggested by Feynman⁷⁸, quantum computers could provide accurate solutions to the many-electron problem, with potential for quantum advantage. Quantum phase estimation (QPE) illustrates the potential,⁷⁹ but requires circuit depths and gate counts that are non-viable on today’s NISQ hardware. This has catalyzed the development of more noise-tolerant algorithms, such as the variational quantum eigensolver (VQE)^{80–83} and a host of improved VQE approaches; see refs. 84 and 85 for recent reviews. While the promise of quantum computing is bright, present-day and near-term hardware limitations preclude applications that are not readily performed on classical hardware, as is apparent from recent reviews.^{86–88} There is hence ample reason to seek improved classical algorithms until the era of quantum utility for strong correlations is demonstrated.

Separate from selected CI or DMRG within an active space for CASSCF, one can seek well-defined polynomial-scaling approximations to the CAS problem instead of trying to solve it exactly. One class of such examples begins with perfect pairing (PP) valence bond (VB) theory,^{89,90} and the CC-VB methods^{91–97} that approximate spin-coupled VB (SC-VB).^{98,99} by limiting non-orthogonality to within a pair, and using a special cluster expansion inspired by projected Hartree-Fock. A related set of examples are the more general geminal-based methods,^{100–105} as well as minimal matrix product states.¹⁰⁶ Additionally one can make coupled-cluster approximations to the active space wave function,^{107–115} although relatively high order truncations are required to achieve useful accuracy for problems with strong correlation character involving more than a single pair of electrons.

To include higher substitutions with lower cost in a coupled-cluster active space model, a family of generalized perfect pairing (PP) models has been proposed. This hierarchy is an alternative way of truncating the coupled-cluster equations to an active space of N electron pairs, or $2N$ electrons in $2N$ orbitals, commonly denoted as $(2N_e, 2N_o)$. To achieve further compactness, the active space in the PP hierarchy is then further assumed to be formed of n pairs of electrons, each doubly occupied orbital being associated with a corresponding virtual orbital.^{116–118} This truncation should be contrasted to the conventional truncation based on the global excitation level as in CC singles and doubles (CCSD), for example.

Following the aforementioned description, the PP version^{89,90,119–122} includes one doubles amplitude per pair of electrons, and is exact (it agrees with CAS) for a single pair of electrons, or a set of non-interacting pairs; the variant of Lehtola, Parkhill, and Head-Gordon¹¹⁸ can also include two single excitation operators corresponding to the spin-up and spin-down excitations. The perfect quadruples model¹¹⁶ is a truncation of CC with singles through quadruples (CCSDTQ) with a quadratic number of amplitudes that yields exactness for 4 electrons in 4 orbitals, or a set of non-interacting 4-electron-in-4-orbital systems. Similarly the perfect hexuples model¹¹⁷ is a truncation of CC with single through hextuple excitations (CCSDTQ56) with a cubic number of amplitudes that is exact for 6 electrons in 6 orbitals, or a set of non-interacting 6-electrons-in-6-orbital systems. We have recently reported efficient implementations of the PQ and PH models including orbital optimization for problem sizes as large as $(228e, 228o)$.^{118,123}

However, generalized PP models have been presented to date only for molecules with singlet ground states. The purpose of this work is to explore extending the PP, PQ, and PH hierarchy to the ground state of systems with a set of N electron pairs, and R radical electrons, such that $M_S = R$ and $S = R/2$. The major question therein is how to generalize the exactness property to radical electrons. Let us illustrate this problem with $R = 1$ odd electron (*i.e.* $S = 1/2$). The simplest alternative is to leave the radical orbital uncorrelated unlike the active electron pairs, which is straightforward albeit unappealing, as it will degrade exactness to the level of just 1 electron for each model—same as Hartree–Fock. It is more logical, but slightly more complicated, to preserve a reduced level of accuracy: 1 electron at the PP level (the radical is unentangled), 3 electrons at the PQ level (the radical is entangled with each electron pair), and 5 electrons at the PH level (the radical is entangled with pairs of pairs). The most ambitious, and most complicated possibility is to provide an *enhanced* level of accuracy: 3, 5, and 7 electrons at PP, PQ, and PH level, respectively. In this work, we will develop all three possibilities, as described in detail in section II.

The implementation, described in section III, makes use of a computer-based algebra generator for high-order coupled-cluster theory, as well as our efficient code generator that translates the sparse tensor contractions into a vectorized form that can be efficiently evaluated.

We then turn to evaluating the three classes of pairing models for radicals on some realistic systems. The computational details are discussed in section IV. Small molecules are not good choices to examine, because there is no reason to use an inexact model. We therefore select polyenes and polyenyl radicals as well as their anions and cations as interesting classes of systems that have non-trivial electron correlation effects. They have been widely studied by multireference methods,^{124,125} a variety of methods by Bally, Hrovat, and Thatcher Borden¹²⁶, DMRG,^{127,128}

SC-VB¹²⁹, classical VB,^{130,131} CC and related methods,¹³² scaled opposite-spin orbital-optimized MP2,¹³³ adaptive CI,¹³⁴ *etc.*. Relevant observables that are sensitive to the accurate treatment of paired *vs.* radical electrons include spin gaps, and ionization energies, all of which are reported on in section V. Our study concludes with a summary and brief discussion in section VI.

II. THEORY

A. The PP, PQ, and PH models

As already mentioned in section I, the PP, PQ, and PH models all use a pairing active space, in which each occupied orbital, i , has a single correlating virtual orbital, i^* , as illustrated in fig. 1. Let us first consider the CC version^{121,122} of the PP model, which is exact for isolated pairs. Here, we thus consider single excitations from the occupied alpha and beta orbitals i and \bar{i} to the corresponding virtuals i^* and \bar{i}^* , respectively, and the double excitation from the occupied alpha and beta orbitals i and \bar{i} to the corresponding virtuals i^* and \bar{i}^* , the overbar denoting beta spin. Although the singles excitation amplitudes are not traditionally considered within PP, we have shown them to be important even at optimal orbitals¹²³ as previously suggested by Köhn and Olsen¹³⁵.

To illustrate the truncation, we will consider the opposite-spin block of the double excitation amplitudes tensor, which is approximated in PP as¹¹⁸

$$(t_{\text{PP}})_{ij}^{ab} = \sum_{p=1}^N t_{pp}^{pp} \delta_{ip} \delta_{jp} \delta_{ap} \delta_{bp}. \quad (1)$$

The $O(N^4)$ amplitudes of CCSD are thereby reduced to N non-zero values in PP, even though exactness within (2e,2o) active spaces and size-consistency are unaffected. In the PQ model,¹¹⁶ all CC terms coupling two pairs are retained to ensure accuracy for 4 electrons in 4 orbitals (*i.e.* 2 pairs) while maintaining the size-consistency of CC. Thus, quadratic subsets (“2P”) of the singles, doubles, triples and quadruples amplitudes are retained in PQ such that

$$\mathbf{t}_{\text{PQ}} = \mathbf{t}_{\text{PP}} + \mathbf{t}_{2\text{P}} \quad (2)$$

For instance, to compare with PP and eq. (1), $\mathbf{t}_{2\text{P}}$ for the opposite-spin block of the double excitation amplitudes tensor is defined as¹¹⁸

$$\begin{aligned} (t_{2\text{P}})_{ij}^{ab} = & \sum_{\substack{p,q=1 \\ p \neq q}}^N t_{pp}^{pq} \delta_{ip} \delta_{jp} \delta_{ap} \delta_{bq} + \sum_{\substack{p,q=1 \\ p \neq q}}^N t_{pp}^{qp} \delta_{ip} \delta_{jp} \delta_{aq} \delta_{bp} + \sum_{\substack{p,q=1 \\ p \neq q}}^N t_{pq}^{pp} \delta_{ip} \delta_{jq} \delta_{ap} \delta_{bp} \\ & + \sum_{\substack{p,q=1 \\ p \neq q}}^N t_{qp}^{pp} \delta_{iq} \delta_{jp} \delta_{ap} \delta_{bp} + \sum_{\substack{p,q=1 \\ p \neq q}}^N t_{pq}^{pq} \delta_{ip} \delta_{jq} \delta_{ap} \delta_{bq} + \sum_{\substack{p,q=1 \\ p \neq q}}^N t_{qp}^{pq} \delta_{iq} \delta_{jp} \delta_{ap} \delta_{bq} + \sum_{\substack{p,q=1 \\ p \neq q}}^N t_{pp}^{qq} \delta_{ip} \delta_{jp} \delta_{aq} \delta_{bq}. \end{aligned} \quad (3)$$

There are corresponding $\mathbf{t}_{2\text{P}}$ terms for the same spin doubles, as well as the various spin blocks of the single, triple, and quadruple substitutions. Overall, the $O(N^8)$ amplitudes of active space CCSDTQ are thereby reduced to $O(N^2)$ non-zero values in PQ, while exactness within (4e,4o) active spaces and size-consistency are unaffected.

To define the PH model¹¹⁷ which is exact for 3 pairs or (6e,6o) active spaces, we introduce a similar equation that contains the additional terms beyond PQ that couple 3 electron pairs (“3P”). This defines the sparsity pattern of the amplitude tensors in the PH method as

$$\mathbf{t}_{\text{PH}} = \mathbf{t}_{\text{PQ}} + \mathbf{t}_{3\text{P}} \quad (4)$$

Again, as an example, $\mathbf{t}_{3\text{P}}$ for the the opposite-spin block of the double excitation amplitudes tensor is defined as:

$$\begin{aligned} (t_{3\text{P}})_{ij}^{ab} = & \sum_{\substack{p,q,r=1 \\ p \neq q \neq r}}^N t_{pp}^{qr} \delta_{ip} \delta_{jp} \delta_{aq} \delta_{br} + \sum_{\substack{p,q,r=1 \\ p \neq q \neq r}}^N t_{qr}^{pp} \delta_{iq} \delta_{jr} \delta_{ap} \delta_{bp} + \sum_{\substack{p,q,r=1 \\ p \neq q \neq r}}^N t_{pq}^{pr} \delta_{ip} \delta_{jq} \delta_{ar} \delta_{bp} \\ & + \sum_{\substack{p,q,r=1 \\ p \neq q \neq r}}^N t_{pq}^{rp} \delta_{ip} \delta_{jq} \delta_{ar} \delta_{bp} + \sum_{\substack{p,q,r=1 \\ p \neq q \neq r}}^N t_{qp}^{pr} \delta_{iq} \delta_{jr} \delta_{ap} \delta_{br} + \sum_{\substack{p,q,r=1 \\ p \neq q \neq r}}^N t_{qp}^{rp} \delta_{iq} \delta_{jr} \delta_{ap} \delta_{br} \end{aligned} \quad (5)$$

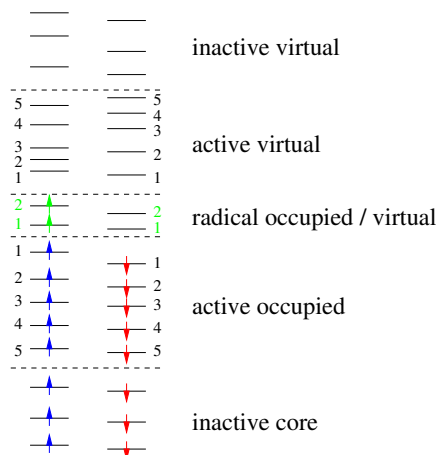


Figure 1: Illustration of the division of the pairing orbital space, including the new unpaired radical class of electrons and orbitals. The example features a (12e,12o) problem for a triplet state, in which the active space is split up into a traditional (10e,10o) perfect pairing active space and a (2e,2o) radical subspace. The radical pairing models are formed by selecting suitable active space truncations of the coupled cluster models.

To ensure exactness for 3 pairs, PH has a large number of other sparse tensors with a cubic number of amplitudes (from 3 pair indices) all the way through hextuple substitutions. Overall, the $O(N^{12})$ amplitudes of active space CCSDTQ56 are thereby reduced to $O(N^3)$ non-zero values in PH, while exactness within (6e,6o) active spaces and size-consistency are again unaffected.

B. The PPr, PQr and PHr models

As discussed in ref. 118, the representation in eqs. (1) to (5) contains an inherent assumption that the active orbital blocks are of equal size. Let us now remove that assumption and instead allow the presence of a set of R radical orbitals, each accompanied by a radical electron. The resulting nominal ground state determinant is illustrated in fig. 1. How should the opposite-spin block of the double excitation amplitudes tensor (and its other spin blocks and other relevant tensors) be approximated now? As foreshadowed in the Introduction, there are three possibilities. The first possibility is the trivial generalization that leaves the definitions of the PP, PQ, and PH sparse amplitude tensors unmodified in their form discussed above for radicals. Therefore, no radical orbitals enter these models, and obviously, no modifications to the equations are required; however, the radical electrons are not correlated and the models lose their exactness properties.

Any other alternative must include additional terms involving, that is, entangling, the radical orbitals and electrons with the paired electrons. The simplest logical way to do this is to include additional terms that have no more labels (either pair or radical labels) than the base model, which defines our second class of candidate open shell models. We shall denote such models as PPr, PQr, and PHr, where the suffix “r” denotes the fact that they are generalizations for molecules with radical electrons. We can write the following relations to define these models:

$$\mathbf{t}_{\text{PPr}} = \mathbf{t}_{\text{PP}} \quad (6)$$

$$\mathbf{t}_{\text{PQr}} = \mathbf{t}_{\text{PPr}} + \mathbf{t}_{2\text{P}} + \mathbf{t}_{2\text{r}} \quad (7)$$

$$\mathbf{t}_{\text{PHr}} = \mathbf{t}_{\text{PQr}} + \mathbf{t}_{3\text{P}} + \mathbf{t}_{3\text{r}} \quad (8)$$

The equivalence of PP and PPr follows from the fact that any correlation between electron pairs and radicals (r) must involve a minimum of two indices: one for the radical label and one for the pair label. This minimal coupling defines the additional $\mathbf{t}_{2\text{r}}$ terms that augment the PQr model relative to PQ. Likewise, $\mathbf{t}_{3\text{r}}$ is defined by amplitudes that entangle 3 different indices, at least one of which is a radical index, and these terms augment the PHr model relative to PH.

For concrete illustration of $\mathbf{t}_{2\text{r}}$ and $\mathbf{t}_{3\text{r}}$, let us again focus on the opposite-spin block of the double excitation amplitudes tensor. At the 2r level, one pair index and one radical index can now entangle so that 3 new terms are retained:

$$(t_{2r})_{ij}^{ab} = \sum_{p=1}^N \sum_{x=1}^R t_{xp}^{pp} \delta_{ix} \delta_{jp} \delta_{ap} \delta_{bp} + \sum_{p=1}^N \sum_{x=1}^R t_{pp}^{px} \delta_{ip} \delta_{jp} \delta_{ap} \delta_{bx} + \sum_{p=1}^N \sum_{x=1}^R t_{xp}^{px} \delta_{ix} \delta_{jp} \delta_{ap} \delta_{bx} \quad (9)$$

As a reminder, these additional terms denote the excitations $(x, \bar{i}) \rightarrow (i^*, \bar{i}^*)$ (radical electron to paired virtual), $(i, \bar{i}) \rightarrow (i^*, \bar{x})$ (paired electron to radical virtual), and $(x, \bar{i}) \rightarrow (i^*, \bar{x})$ (radical electron to paired virtual, and paired electron to radical virtual). At the level of 3 entangled indices, two pair indices and one radical index, or one pair index and two radical indices can be entangled, giving rise to the following additional terms

$$\begin{aligned} (t_{3r})_{ij}^{ab} = & \sum_{\substack{p,q=1 \\ p \neq q}}^N \sum_{x=1}^R t_{xq}^{pp} \delta_{ix} \delta_{jq} \delta_{ap} \delta_{bp} + \sum_{p=1}^N \sum_{\substack{x,y=1 \\ x \neq y}}^R t_{xp}^{py} \delta_{ix} \delta_{jp} \delta_{ap} \delta_{by} + \sum_{\substack{p,q=1 \\ p \neq q}}^N \sum_{x=1}^R t_{xp}^{pq} \delta_{ix} \delta_{jp} \delta_{ap} \delta_{bq} \\ & + \sum_{\substack{p,q=1 \\ p \neq q}}^N \sum_{x=1}^R t_{xq}^{px} \delta_{ix} \delta_{jq} \delta_{ap} \delta_{bx} + \sum_{\substack{p,q=1 \\ p \neq q}}^N \sum_{x=1}^R t_{xp}^{qp} \delta_{ix} \delta_{jp} \delta_{aq} \delta_{bp} + \sum_{\substack{p,q=1 \\ p \neq q}}^N \sum_{x=1}^R t_{pq}^{px} \delta_{ip} \delta_{jq} \delta_{ap} \delta_{bx} \\ & + \sum_{\substack{p,q=1 \\ p \neq q}}^N \sum_{x=1}^R t_{qp}^{px} \delta_{iq} \delta_{jp} \delta_{ap} \delta_{bx} + \sum_{\substack{p,q=1 \\ p \neq q}}^N \sum_{x=1}^R t_{pp}^{qx} \delta_{ip} \delta_{jp} \delta_{aq} \delta_{bx} \end{aligned} \quad (10)$$

that correspond to the $(x, \bar{j}) \rightarrow (i^*, \bar{i}^*)$, $(x, \bar{i}) \rightarrow (i^*, \bar{y})$, $(x, \bar{i}) \rightarrow (i^*, \bar{j}^*)$, $(x, \bar{j}) \rightarrow (i^*, \bar{x})$, $(x, \bar{i}) \rightarrow (i^*, \bar{j}^*)$, $(i, \bar{j}) \rightarrow (i^*, \bar{x})$, $(j, \bar{i}) \rightarrow (i^*, \bar{x})$, and $(i, \bar{i}) \rightarrow (j^*, \bar{x})$ excitations, i and j denoting pair indices and x and y denoting radical indices.

Let us briefly consider the exactness properties of the PPr, PQr and PHr models. For PPr, exactness is maintained for isolated pairs of electrons (not just singlets but also triplets in a trivial fashion, because there are no empty α orbitals), as well as isolated radicals. However, a three-electron doublet fragment cannot be exact, although a quartet three-electron fragment is trivially exact. Moving on to PQr, the structure of the additional terms makes it clear that PQr will be exact for doublet three-electron systems, and non-interacting clusters of three-electron and four-electron systems, including triplet fragments, and subsets thereof. Finally, it is evident that PHr will be exact for five-electron doublet or higher-spin systems, and non-interacting clusters of five- and six-electron systems, and subsets thereof. In summary, for doublet systems, this hierarchy of radical models is exact for $(2n - 1)$ electron systems ($n = 1, 2, 3$ for PPr, PQr, and PHr) in the pairing active space, and exact for $2n$ -electron singlet and triplet multiplicities.

C. The PPxr, PQxr and PHxr models

There is another possible generalization of the pairing models to radical systems that has more desirable exactness properties than the models introduced above. Let us recall that the \mathbf{t}_{2r} terms were added to the base PQ model to define the PQr model via eq. (7), while the PPr model was unchanged from PP itself. We can instead augment the PP model itself with the \mathbf{t}_{2r} to yield a version of PP with extended radical (xr) correlations:

$$\mathbf{t}_{\text{PPxr}} = \mathbf{t}_{\text{PP}} + \mathbf{t}_{2r} \quad (11)$$

From the previous subsection, we recall that the \mathbf{t}_{2r} terms entangle radicals with pairs (e.g. as illustrated in eq. (9) for the opposite-spin block of the double excitation amplitudes). By definition there must be at least one radical index, which means that there is at most one pair index in each amplitude in \mathbf{t}_{2r} . Thus inclusion of these one-pair index radical correlations in the PPxr model is consistent with the inclusion of only one-pair correlations in PP itself. Furthermore, if we are interested in the doublet manifold, we note that $R = 1$ for all doublet states and therefore the number of retained amplitudes in \mathbf{t}_{2r} is only $3N$, similar to the N amplitudes contained in \mathbf{t}_{PP} .

In the same spirit, it would also be possible to include terms of the type $(x, \bar{i}) \rightarrow (i^*, \bar{y})$ in an extended PP model with $O(N)$ amplitudes; however, for simplicity, we will restrict the number of radical indices similarly to the pair indices, allowing up to 2 radical indices for PQxr and up to 3 radical indices for PHxr. Now, inductive generalization suggests that PQxr and PHxr models should be defined as follows:

$$\mathbf{t}_{\text{PQxr}} = \mathbf{t}_{\text{PPxr}} + \mathbf{t}_{2P} + \mathbf{t}_{3r} + \mathbf{t}_{4r} \quad (12)$$

$$\mathbf{t}_{\text{PHxr}} = \mathbf{t}_{\text{PQxr}} + \mathbf{t}_{3P} + \mathbf{t}_{5r} + \mathbf{t}_{6r} \quad (13)$$

	t/λ
PP (and PPr)	$3N$
PPxr	$3N + 5NR$
PQ	$3N + 16N^2$
PQr	$3N + 5NR + 16N^2$
PQxr	$3N + 5NR + NR^2 + 16N^2 + 27N^2R + 20N^2R^2$
	γ
PP (and PPr)	$6N$
PPxr	$2R + 6N + 6NR$
PQ	$6N + 6N^2$
PQr and PQxr	$2R + 2R^2 + 6N + 6NR + 6N^2$
	Γ
PP (and PPr)	$13N$
PPxr	$R + 13N + 55NR$
PQ	$13N + 105N^2$
PQr	$R + 5R^2 + 13N + 55NR + 105N^2$
PQxr	$R + 9R^2 + 13N + 57NR + 49NR^2 + 105N^2 + 117N^2R + 31N^2R^2$

Table I: Storage costs for the t and λ amplitudes, and the one- and two-electron density matrices γ and Γ , respectively, that appear in some of the models considered in the present work, in terms of the number of electron pairs, N , and the number of unpaired radical electrons, R .

In direct analogy to the discussion above for PPxr, the \mathbf{t}_{3r} and \mathbf{t}_{4r} terms now incorporated into PQxr include no more than two pair indices, just like the parent PQ model itself; however, up to two radical indices can be included, leading to a maximum of 4 indices in the subtensor. Likewise the \mathbf{t}_{5r} and \mathbf{t}_{6r} terms incorporated into PHxr include correlations between radical and pair indices so that no more than three pair indices can appear just like in the parent closed-shell PH model, but in addition up to three radical indices can be included, yielding up to six indices in total.

Let us next consider the exactness properties of the PPxr, PQxr and PHxr models. For PPxr, exactness is of course maintained for isolated pairs of electrons (both singlets and triplets) as discussed above in section II B for PPr which is a subset of PPxr. In contrast to PPr, three-electron doublet fragments are also exact in PPxr, due to inclusion of the \mathbf{t}_{2r} terms. Note that triple substitutions are not necessary for (3e,3o) exactness as there is only one α virtual, and only one β occupied. Therefore, like PP and PPr, PPxr is a subset of CCSD. It is interesting to note that PPxr is also exact for the (4e,4o) triplet, the (5e, 5o) quartet, *etc.*, each of which also requires only double substitutions.

Moving on to PQxr, the structure of the additional terms mandates that the model is exact for doublet 5 electron systems, while PQr was only exact for doublet 3 electron systems. Quintuple substitutions are not necessary for (5e,5o) exactness, so PQxr is a subset of active-space CCSDTQ like PQ and PQr. Similarly PQxr is exact for non-interacting clusters of five electrons, and other four-electron clusters due to its size-consistency. PQxr is also exact for six-electron triplets, seven-electron quartets *etc.*, while still being a subset of CCSDTQ like PQr. Finally, PHxr is exact for seven-electron doublet (or higher-spin) systems, and non-interacting clusters of seven- and six-electron systems, and subsets thereof, all while still being a subset of CCSDTQ56 like its corresponding closed-shell PH parent model and the PHr model.

This kind of truncation then yields (3e,3o) exactness for PPxr, the (6e,6o) triplet for PQxr, and the (9e,9o) quintet for PHxr, and subsets thereof.

III. IMPLEMENTATION

The implementation of the new models is done using the same framework and automatic code generator as in ref. 118, which proceeds briefly as follows. Starting from the standard CC equations in spin-orbital form that have been generated with a computer algebra system,¹³⁶ the spin is integrated out to obtain the equations in terms of the various spin blocks of the (de-)excitation tensors, the integrals and the density matrices. Next, the decompositions for the spin blocks, exemplified by eqs. (1), (3), (9) and (10) *etc.*, are generated, and summations over the Kronecker symbols are performed in the CC equations. This yields the equations for the pairing models in terms of the dense subtensors

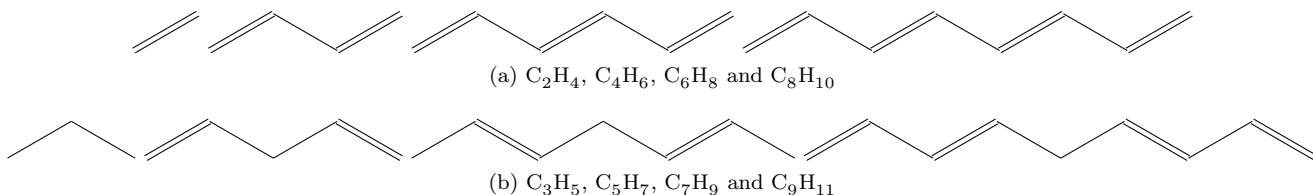


Figure 2: Illustration of the used model geometries for the polyenes and polyenyls; larger molecules are obtained by continuation of the series. The single and double lines denote single and double bonds, whose bond lengths are given in the main text.

only. Finally, the generator writes out C++ code that implements the equations. The resulting storage costs for the t excitation amplitudes, the λ de-excitation amplitudes, and the one- and two-electron density matrices are given in table I.

Due to the significant number of additional terms that arise from the presence of radical orbitals, in the present work we will only consider the full PPxr and PQxr models, and the CCSDTQ subset of PHr and PHxr. The code generator at its present stage of development cannot feasibly form the terms needed for the full models, as the number of possible labelings grows exponentially in the order of the original tensors, and the tensor product pairing algorithm is cubic scaling in the number of labelings. A complete refactor (rewrite) of the proof-of-concept pairing code generator is expected to make generating the full PHxr model tractable, but this undertaking is beyond the scope of the present proof-of-concept work. The partial implementation of the radical PH models will be denoted as PHrQ or and PHxrQ to indicate that only terms through quadruples are retained. The partial implementation of the PH model is analogously denoted as PHQ.

The radical models are generated with two-pair, three-pair, and four-pair intermediates for PP, PQ and PH level, respectively. That choice is in accordance to the truncation scheme chosen in section II. For instance the two-pair intermediates of PPxr may have up to two pair labels as well as up to two radical orbital labels.

IV. COMPUTATIONAL DETAILS

In the present work, we study polyene and polyenyl molecules at fixed model geometries. Following Hachmann, Cardoen, and Chan¹²⁷ the polyene geometries are extracted from density functional calculations extrapolated to the bulk limit,¹³⁷ yielding the parameters $R(C=C) = 1.3693 \text{ \AA}$, $R(C-C) = 1.4244 \text{ \AA}$, and $R(C-H) = 1.0820 \text{ \AA}$, with all bond angles equalling 120° and the molecules being planar. In the present work, for simplicity, the same parameters are also used for the polyenyls. To account for the polyenyls' radical character, the polyenyls are constructed to contain two single bonds at the middle of the molecule to host the radical electron. The molecular structures are illustrated in fig. 2. Both polyenes and polyenyls possess C_s symmetry; symmetry restrictions were, however, not imposed in the calculations.

The automatically generated pairing models have been interfaced with the ERKALE program,^{138,139} which is used to generate the integrals and perform the orbital optimization with the geometric direct minimization (GDM) method^{140–142} in which the descent direction is determined by a Broyden–Fletcher–Goldfarb–Shanno (BFGS) algorithm¹⁴³ preconditioned with diagonal second derivatives, and the optimization is continued until the norm of the orbital gradient satisfies $\|\partial\mathcal{L}/\partial\theta_{pq}\| < 10^{-5}$.

The cc-pVDZ basis set¹⁴⁴ is employed in all calculations, and the pairing active space is used for all valence electrons. That is, a full valence space of $((5n+2)e, (5n+2)o)$ is used for for the C_nH_{n+2} neutral species, whereas for cationic species the active space is reduced to a quasi-full-valence $((5n+1)e, (5n+1)o)$ active space. Thus, the active spaces range from $(11e, 11o)$ for $C_2H_4^+$ to $(122e, 122o)$ for $C_{22}H_{24}$. Note that the size of the active space is the same regardless of the studied spin state, but the composition of the active space does depend on the number of unpaired electrons. Single-point calculations are run with the PP, PPr, PPxr, PQ, PQr, PQxr, PHQ, PHrQ, and PHxrQ models up through $C_{16}H_{18}$ *i.e.* active spaces up to $(82e, 82o)$. All the single-point calculations include single excitations within the active space, allowing the orbitals to relax within the active space.

As in our previous work,¹²³ the calculations are initialized using ROHF electron densities. A suitable initial guess is generated by localizing the occupied orbitals¹⁴⁵ using the generalized Pipek–Mezey criterion¹⁴⁶ using Becke charges. The generalized Pipek–Mezey localization is run separately for the paired active space and for the radical orbitals, after which corresponding virtual orbitals are generated for the paired active orbitals using the Sano guess.^{141,147} Two-electron integrals and Fock matrices are evaluated using the Cholesky decomposition method,^{148,149} following the approach of ref. 150 with a 10^{-10} integral screening threshold and a 10^{-9} threshold for the Cholesky procedure

n_C	PP	PQ	PHQ	PQr	PHrQ	PPxr	PQxr	PHxrQ	MRMP ^a	expt. ^b
2	3.971	4.509	4.585	4.387	4.399	3.869	4.295	4.375		4.32-4.36 ^b
4	3.554	4.327	4.516	3.455	3.322	2.805	3.106	3.210	3.20	3.22 ^c
6	3.361	4.327	4.576	3.268	2.820	2.527	2.511	2.626	2.40	2.58-2.61 ^d
8	3.327	4.357	4.742	3.044	2.513	2.231	2.039	2.234	2.20	2.10 ^e
10	3.268	4.403	4.809	3.051	2.334	2.162	1.819	2.003	1.89	
12	3.293	4.414	4.865	3.036	2.289	2.150	1.699	1.890		
16	3.280	4.433	4.912	3.049	2.231	2.130	1.602			
20	3.276	4.439	4.926	3.052		2.125	1.576			

^a Multireference perturbation theory calculations from ref. 124.

^b Experimental value from refs. 151 and 152.

^c Experimental value from refs. 153 and 154.

^d Experimental value from refs. 155–157.

^e Experimental value from ref. 158.

Table II: Singlet-triplet gaps for polyenes in eV using RO-PPxr orbitals.

itself.

Since orbital optimization is only practical for large calculations with the basic PP model and its PPxr extension, we must make a choice of which model to use for assessments of energy differences such as spin gaps and ionization energies. To ensure spin-pure states, we choose to use restricted orbitals (RO), and to include some correlation effects associated with the radical orbitals we use the PPxr model to optimize the orbitals. Thus all single-point energy differences reported in the following section employ RO-PPxr optimized orbitals, together with the standard geometries discussed above, and the cc-pVDZ basis set.

V. RESULTS

A. Singlet-triplet gaps of polyenes

Vertical singlet-triplet (ST) gaps for the polyenes are given in table II. Calculated ST gaps are an interesting measure of balance in the treatment of differential correlation effects when the pairing of two electrons is disrupted. In our context, the PP, PQ and PHQ models *clearly undercorrelate* the radical electrons of the triplet. This trend is expected: since the radical orbitals do not enter any amplitudes, the radical orbitals are not correlated at all. The trend is manifested in the *strongly increasing* ST gaps for the PP, PQ, PHQ sequence, where pair correlations are increasingly complete, whilst the radical orbitals remain uncorrelated.

The r and xr models may then offer potentially more balanced treatments of two electrons that are paired versus unpaired. This improved balance is evident in the results of table II, as much smaller changes occur across the PP, PQ, PH sequence for the r and xr models. While our calculations use model geometries, and are performed only in the quasi-full-valence active space, it is evident that PPxr, and particularly PQxr and PHxrQ compare very well with both experimental values, and with multireference Møller–Plesset (MRMP) reference values. The dramatic improvement of PPxr relative to PP is noteworthy. It is also noteworthy that the values for PQxr agree much better with the reference values for the longer chains than the ones for PQr. Finally, only very small changes are seen moving from PQxr to PHxrQ, which is the most complete method implemented here. All these observations suggest that the xr models are significantly better balanced than the r models.

B. Ionization energies of polyenes

Ionization energies in the polyenes are another interesting test of the balance that various computational models can achieve for electron correlation effects in doublet radical cations versus closed shell neutrals. While modern DFT is generally acceptable for ionization energies, DFT results for polyenes are considered unreliable in general, because polyenes are known to exhibit strong static correlation,^{118,127,128} and because DFT results for these systems exhibit a strong dependence on the fraction of exact exchange, which is often a symptom of delocalization error.¹⁵⁹

Pairing method calculations for the first vertical ionization energies of the polyenes are shown in table III, again in the quasi-full-valence active space. They are compared against experimental values^{160–166} for the shorter polyenes,

n_C	PP	PQ	PHQ	PQr	PHrQ	PPxr	PQxr	PHxrQ	CCSD(T) ^a	expt.
2	9.528	10.078	10.154	10.056	10.127	9.508	10.049	10.126		10.51 ^b
4	8.490	9.374	9.562	9.103	8.981	8.213	8.791	8.903	9.27	9.08 ^c
6	7.883	8.822	9.089	8.379	8.206	7.418	7.930	8.091		8.29-8.30 ^d
8	7.569	8.603	8.870	8.132	7.827	7.081	7.536	7.676	7.93	7.79 ^e
12	7.182	8.310	8.581	7.814	7.364	6.676	7.051	7.159	7.32	
16	6.998	8.178	8.431	7.681	7.138	6.491	6.832	6.893	6.96	
20	6.905	8.118	8.348	7.621		6.398	6.728		6.74	
24	6.857	8.090		7.593		6.350	6.676		6.57	

^a DLPNO-CCSD(T) calculations extrapolated to the basis set limit from ref. 167.

^b Experimental value from refs. 160–162.

^c Experimental value from ref. 163.

^d Experimental value from refs. 164 and 165.

^e Experimental value from ref. 166.

Table III: First ionization energies of polyenes in eV using RO-PPxr orbitals.

n_C	PP	PQ	PHQ	PQr	PHrQ	PPxr	PQxr	PHxrQ	CASPT2 ^a	expt. ^b
3	4.691	5.131	5.190	5.330	5.562	4.905	5.460	5.585	5.89	6.33
5	4.779	5.377	5.497	5.319	5.083	4.755	4.930	4.978		
7	2.917	3.705	3.960	3.174	3.227	2.469	2.926	3.140		

^a Calculation from ref. 168.

^b Experimental value from ref. 169.

Table IV: Doublet-quadruplet gaps for polyenyls in eV using RO-PPxr optimized orbitals.

as well as against domain localized pair natural orbital CCSD(T) [DLPNO-CCSD(T)] calculations¹⁶⁷ for the longer chain species. Although the DLPNO-CCSD(T) calculations are extrapolated to the complete basis set limit while the pairing active space calculations exclude most dynamic correlations, it is nevertheless striking that PQxr and PHxr agree roughly equally well with experiment as the much more expensive CCSD(T) calculations. Unsurprisingly, the simplest methods, PQ and PHQ, are in qualitative disagreement with the higher-level calculations, and are less balanced than PP itself, as they fail to correlate the unpaired electron. Even PQr is in error by roughly 0.8 eV for the longer chain lengths, and it is striking how much better-balanced the PQxr model is relative to the experiment and full coupled-cluster results in these cases.

C. Doublet-quartet gaps of polyenyls

The calculated spin gap between the doublet (ground) state and the quartet (excited) state of the polyenyl series is shown in table IV, as a function of the number of C atoms in the radical chain. These gaps do not appear to have been thoroughly investigated: as far as we are aware, doublet-quartet gaps are only available for C₃H₅ from CASPT2 calculations (ref. 168) and from experiment (ref. 169), and so we only report data for the three smallest polyenyls. Although there is a slight discrepancy from experiment, likely arising from the already mentioned issues of basis set and missing dynamical correlation, the radical models are, however, in good agreement with the CASPT2 value of ref. 168 for C₃H₅. The original PP, PQ, and PHQ models not only show a larger error for C₃H₅, but also do not predict monotonic behavior for the doublet-quartet gap as they do not correlate the radical electrons at all.

Calculations for the first vertical ionization energies of the polyenyls are shown in table V, again in the quasi-full-valence active space. They are compared against experimental values from refs. 170–173. The radical models are once again in good agreement with experiment, showing monotonically decreasing ionization energies with increasing carbon chain length.

n_C	PP	PQ	PHQ	PQr	PHrQ	PPxr	PQxr	PHxrQ	expt.
3	6.996	7.088	7.058	7.506	7.742	7.403	7.773	7.804	8.1 ^a , 8.13 ^b
5	6.043	6.065	5.995	6.692	6.999	6.671	7.081	7.094	7.25 ^c , 7.76 ^d
7	5.544	5.763	5.610	6.374	6.733	6.119	6.894	6.869	
9	5.290	5.307	5.145	6.011	6.412	5.967	6.592	6.558	

^a Experimental value from ref. 170.

^b Experimental value from ref. 171.

^c Experimental value from ref. 172.

^d Experimental value from ref. 173.

Table V: First ionization energies of polyenyls in eV, computed using PPxr orbitals.

D. Optimal orbitals

Finally, in addition to the study of the numerical performance of the models, it is also interesting to examine the resulting orbital picture. The neutral polyenes and charged polyenyl species have singlet ground states in which all electrons are paired. Here, we will examine the orbitals for the unpaired electron in a charged polyene, $C_{20}H_{22}^+$, and a neutral polyenyl radical, $C_{21}H_{23}$.

The unpaired π_u orbital in $C_{20}H_{22}^+$ corresponding to the ROHF, PP, and PPxr levels of theory are shown in fig. 3 using an 85% density containment criterion to define the isosurfaces.^{146,174} The ROHF SOMO is delocalized over the whole chain and has inversion symmetry (a_u irreducible representation) about the center of the molecule, consistent with the C_{2h} nuclear framework symmetry. Additional ROHF calculations followed by stability analysis using Q-Chem¹⁷⁵ confirm that this solution is a local minimum. Surprisingly, even though the unpaired orbital is not correlated at the PP level of theory, PP partially localizes the SOMO around the short C(9)–C(10) bond (numbering the atoms from the left), to cover just over half the chain, while breaking point group symmetry. The PPxr SOMO is relatively little changed from PP. The main visual difference is that it localizes on the short C(11)–C(12) bond. However, that is symmetry equivalent to the C(9)–C(10) bond about which the PP orbital localized. These findings on the degree of localization of the unpaired singly occupied orbital are in good qualitative agreement with a previous study employing the orbital-optimized scaled opposite-spin MP2 method.¹³³

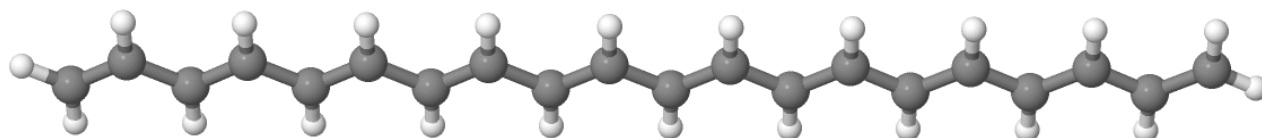
Repeating the demonstration for the unpaired SOMO in $C_{21}H_{23}$ (which has C_{2v} framework symmetry; fig. 2, one obtains the results shown in fig. 4. The ROHF orbital is again delocalized over almost the whole molecule, though to a lesser extent than in the polyene cations. Symmetry is again preserved. In PP and PPxr, the radical electron localizes strongly around the two single bonds at the center of the molecule, the PPxr orbital being slightly less localized as expected due to the correlations with the paired electrons in the model. In contrast to the polyene cation case, the PP and PPxr SOMOs preserve point group symmetry. This reflects our choice of model geometry, which was designed for radicals in the case of the polyenyl chains, but for closed shell neutrals in the polyene chains. Overall both of these examples illustrate the fact that correlation effects induce partial localization of the radical electron relative to mean-field ROHF.

VI. SUMMARY AND DISCUSSION

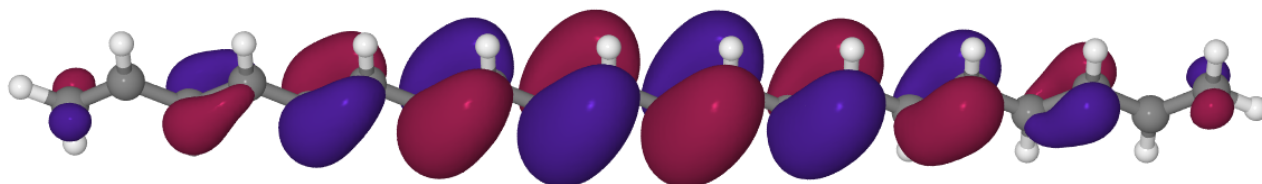
We have presented the extensions of the perfect pairing (PP), the perfect quadruples (PQ) and the CCSDTQ subset of the the perfect hexuples (PH) models to open-shell systems, and demonstrated their accuracy with calculations on the ground, excited and cationic states of polyenes and polyenyls. The results are encouraging, as they indicate the feasibility of accurate yet cost-efficient *ab initio* models for open-shell systems exhibiting strong correlation.

Although the pairing models are limited to symmetric active spaces of N electrons in N orbitals and not all strong correlation problems are amenable to a single-reference coupled-cluster description upon which the pairing models rely,^{123,176} the pairing models are ideal for the description of large hydrocarbons where the natural full-valence active space is N electrons in N orbitals and the strong correlation effects appear to be describable by a truncated CCSDTQ or CCSDTQ56 model as found in this work and refs. 118 and 123.

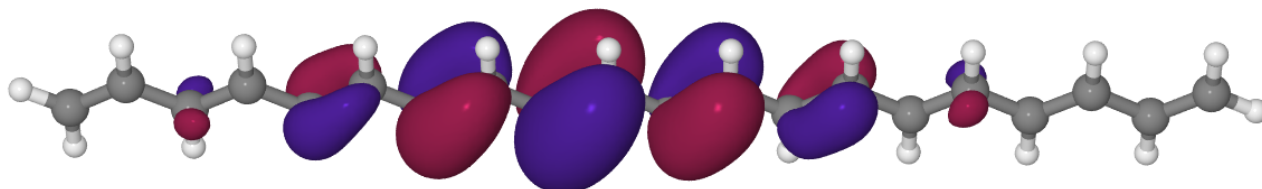
The approach outlined in the present work could also be easily used to extend the pairing models to e.g. asymmetric active spaces by introducing new classes depicting lone electron pairs of electron-rich atoms or vacant orbitals in electron-poor atoms, or further to dynamical correlation by introducing further excitations to the inactive virtual orbitals. While such extensions might be very appealing for applications on chemical problems, the challenge arises in that the favorable scaling of the pairing approaches is destroyed by the additional external labels whose size



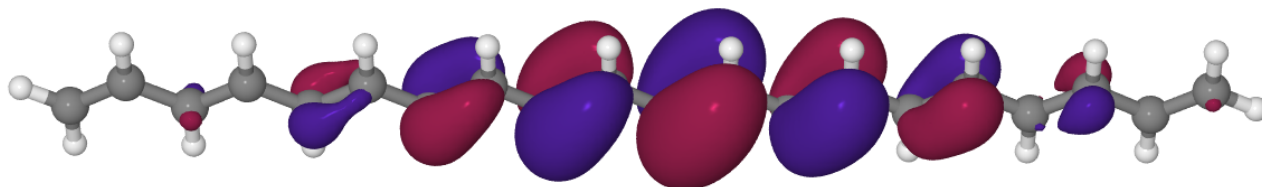
(a) Molecular geometry



(b) ROHF

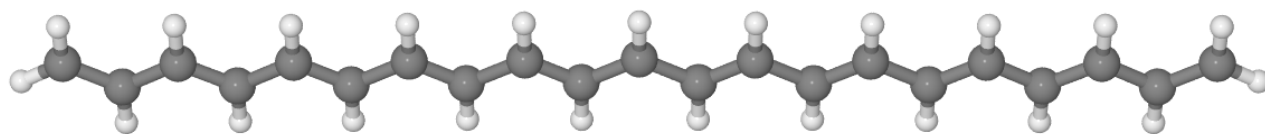


(c) PP

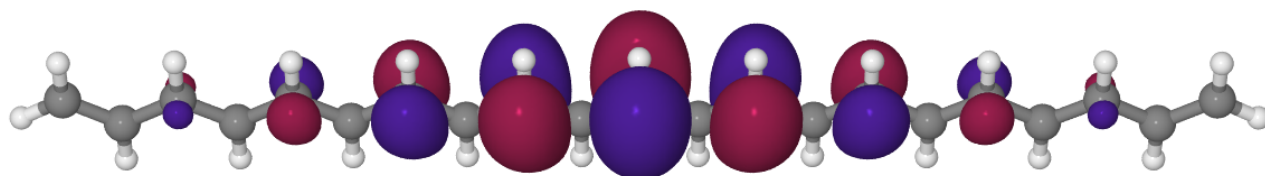


(d) PPxr

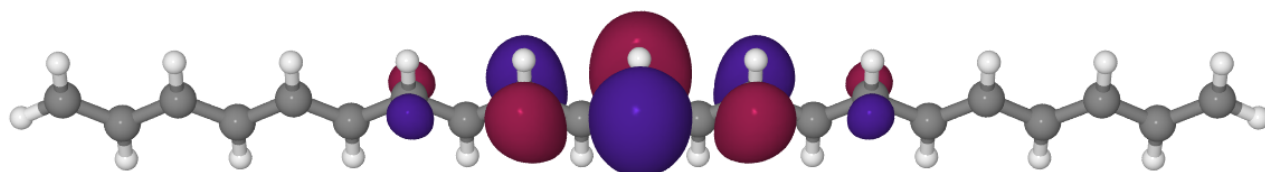
Figure 3: The 85 % density containment plot^{146,174} of the unpaired, singly occupied orbital in C₂₀H₂₂⁺ in the ROHF, PP, and PPxr models. A ROHF calculation with Q-Chem¹⁷⁵ converges to the same energy, and stability analysis showed the ROHF solution to be a proper local minimum.



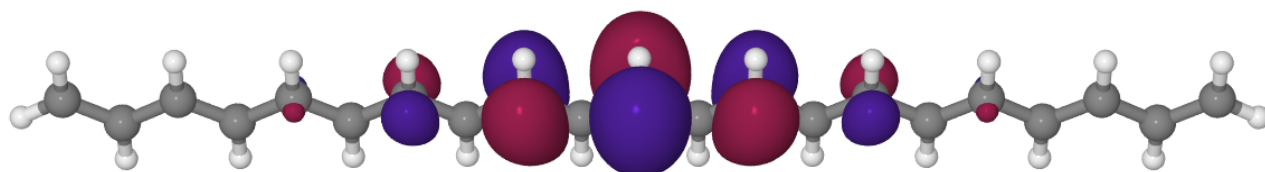
(a) Molecular geometry



(b) ROHF



(c) PP



(d) PPxr

Figure 4: The 85 % density containment plot^{146,174} of the unpaired, singly occupied orbital in C₂₁H₂₃ in the ROHF, PP, and PPxr models. A ROHF calculation with Q-Chem converges to the same energy, and stability analysis showed the ROHF solution to be a proper local minimum.

increase with system size, unlike the present case. In order to tackle these cases, one alternative might be to omit the pairing altogether but restrict the realm of the higher connected excitation operators as in active-space coupled-cluster methods.^{108,109}

As we have numerically demonstrated here and in our previous work,¹²³ orbital-optimized coupled-cluster theory does not converge to the full configuration interaction (FCI) limit in the absence of single excitations.¹³⁵ However, the pairing models are straightforward to extend to a non-orthogonal coupled-cluster treatment which does converge to the FCI limit.¹⁷⁷ Non-orthogonal extensions of the pairing models could be investigated in future work.

ACKNOWLEDGMENTS

This work was supported by the Director, Office of Basic Energy Sciences, Chemical Sciences, Geosciences, and Biosciences Division of the U.S. Department of Energy, under Contract No. DE-AC02-05CH11231, as well as the Academy of Finland under grant numbers 311149, 350282, and 353749. Computational resources provided by CSC – It Center for Science Ltd (Espoo, Finland) and the Finnish Grid and Cloud Infrastructure (persistent identifier urn:nbn:fi:research-infras-2016072533) are gratefully acknowledged.

REFERENCES

- ¹P. Hohenberg and W. Kohn, “Inhomogeneous electron gas,” *Phys. Rev.* **136**, B864–B871 (1964).
- ²W. Kohn and L. J. Sham, “Self-consistent equations including exchange and correlation effects,” *Phys. Rev.* **140**, A1133–A1138 (1965).
- ³N. Mardirossian and M. Head-Gordon, “Thirty years of density functional theory in computational chemistry: an overview and extensive assessment of 200 density functionals,” *Mol. Phys.* **115**, 2315–2372 (2017).
- ⁴L. Goerigk, A. Hansen, C. Bauer, S. Ehrlich, A. Najibi, and S. Grimme, “A look at the density functional theory zoo with the advanced GMTKN55 database for general main group thermochemistry, kinetics and noncovalent interactions,” *Phys. Chem. Chem. Phys.* **19**, 32184–32215 (2017).
- ⁵C. Møller and M. S. M. Plesset, “Note on an approximation treatment for many-electron systems,” *Phys. Rev.* **46**, 618–622 (1934).
- ⁶R. J. Bartlett, “Coupled-cluster theory and its equation-of-motion extensions,” *Wiley Interdiscip. Rev. Comput. Mol. Sci.* **2**, 126–138 (2012).
- ⁷L. Salem and C. Rowland, “The Electronic Properties of Diradicals,” *Angew. Chemie Int. Ed. English* **11**, 92–111 (1972).
- ⁸M. Abe, “Diradicals,” *Chem. Rev.* **113**, 7011–7088 (2013).
- ⁹W. Zhou and J. Liu, “Multi-metal-dependent nucleic acid enzymes,” *Metallomics* **10**, 30–48 (2018).
- ¹⁰K. H. Marti, I. M. Ondák, G. Moritz, and M. Reiher, “Density matrix renormalization group calculations on relative energies of transition metal complexes and clusters,” *J. Chem. Phys.* **128**, 014104 (2008).
- ¹¹C. F. Bender and E. R. Davidson, “Studies in Configuration Interaction: The First-Row Diatomic Hydrides,” *Phys. Rev.* **183**, 23–30 (1969).
- ¹²S. R. Langhoff, S. T. Elbert, and E. R. Davidson, “A configuration interaction study of the spin dipole-dipole parameters for formaldehyde and methylene,” *Int. J. Quantum Chem.* **7**, 999–1019 (1973).
- ¹³B. Huron, J. P. Malrieu, and P. Rancurel, “Iterative perturbation calculations of ground and excited state energies from multiconfigurational zeroth-order wavefunctions,” *J. Chem. Phys.* **58**, 5745–5759 (1973).
- ¹⁴R. J. Buenker and S. D. Peyerimhoff, “Individualized configuration selection in CI calculations with subsequent energy extrapolation,” *Theor. Chim. Acta* **35**, 33–58 (1974).
- ¹⁵R. J. Buenker, S. D. Peyerimhoff, and W. Butscher, “Applicability of the multi-reference double-excitation CI (MRD-CI) method to the calculation of electronic wavefunctions and comparison with related techniques,” *Mol. Phys.* **35**, 771–791 (1978).
- ¹⁶S. Evangelisti, J.-P. Daudey, and J.-P. Malrieu, “Convergence of an improved CIPSI algorithm,” *Chem. Phys.* **75**, 91–102 (1983).
- ¹⁷R. Cimiraglia and M. Persico, “Recent advances in multireference second order perturbation CI: The CIPSI method revisited,” *J. Comput. Chem.* **8**, 39–47 (1987).
- ¹⁸F. Illas, J. Rubio, J. M. Ricart, and P. S. Bagus, “Selected versus complete configuration interaction expansions,” *J. Chem. Phys.* **95**, 1877 (1991).
- ¹⁹R. J. Harrison, “Approximating full configuration interaction with selected configuration interaction and perturbation theory,” *J. Chem. Phys.* **94**, 5021 (1991).
- ²⁰J. Daudey, J. Heully, and J. Malrieu, “Size-consistent self-consistent truncated or selected configuration interaction,” *J. Chem. Phys.* **99**, 1240–1254 (1993).
- ²¹F. Neese, “A spectroscopy oriented configuration interaction procedure,” *J. Chem. Phys.* **119**, 9428–9443 (2003).
- ²²R. Roth, “Importance truncation for large-scale configuration interaction approaches,” *Phys. Rev. C* **79**, 064324 (2009), arXiv:0903.4605.
- ²³Y. Garniron, A. Scemama, E. Giner, M. Caffarel, and P.-F. Loos, “Selected configuration interaction dressed by perturbation,” *J. Chem. Phys.* **149**, 064103 (2018), arXiv:1806.04970.
- ²⁴J. Ivanic and K. Ruedenberg, “Identification of deadwood in configuration spaces through general direct configuration interaction,” *Theor. Chem. Acc.* **106**, 339–351 (2001).
- ²⁵J. Ivanic and K. Ruedenberg, “Deadwood in configuration spaces. II. singles + doubles and singles + doubles + triples + quadruples spaces,” *Theor. Chem. Acc.* **107**, 220–228 (2002).
- ²⁶L. Bytautas and K. Ruedenberg, “A priori identification of configurational deadwood,” *Chem. Phys.* **356**, 64–75 (2009).
- ²⁷J. C. Greer, “Estimating full configuration interaction limits from a Monte Carlo selection of the expansion space,” *J. Chem. Phys.* **103**, 1821 (1995).
- ²⁸J. C. Greer, “Monte Carlo Configuration Interaction,” *J. Comput. Phys.* **146**, 181–202 (1998).
- ²⁹G. H. Booth, A. J. W. Thom, and A. Alavi, “Fermion Monte Carlo without fixed nodes: a game of life, death, and annihilation in Slater determinant space,” *J. Chem. Phys.* **131**, 054106 (2009).
- ³⁰G. H. Booth and A. Alavi, “Approaching chemical accuracy using full configuration-interaction quantum Monte Carlo: a study of ionization potentials,” *J. Chem. Phys.* **132**, 174104 (2010).
- ³¹G. H. Booth, D. Cleland, A. J. W. Thom, and A. Alavi, “Breaking the carbon dimer: the challenges of multiple bond dissociation with full configuration interaction quantum Monte Carlo methods,” *J. Chem. Phys.* **135**, 084104 (2011).
- ³²G. H. Booth and G. K.-L. Chan, “Communication: Excited states, dynamic correlation functions and spectral properties from full configuration interaction quantum Monte Carlo,” *J. Chem. Phys.* **137**, 191102 (2012), arXiv:1210.1650.
- ³³G. H. Booth, A. Grüneis, G. Kresse, and A. Alavi, “Towards an exact description of electronic wavefunctions in real solids,” *Nature* **493**, 365–370 (2012).

- ³⁴N. Ben Amor, F. Bessac, S. Hoyau, and D. Maynaud, "Direct selected multireference configuration interaction calculations for large systems using localized orbitals," *J. Chem. Phys.* **135**, 014101 (2011).
- ³⁵J. J. Shepherd, G. H. Booth, and A. Alavi, "Investigation of the full configuration interaction quantum Monte Carlo method using homogeneous electron gas models." *J. Chem. Phys.* **136**, 244101 (2012).
- ³⁶J. J. Shepherd, A. Grüneis, G. H. Booth, G. Kresse, and A. Alavi, "Convergence of many-body wave-function expansions using a plane-wave basis: From homogeneous electron gas to solid state systems," *Phys. Rev. B* **86**, 035111 (2012).
- ³⁷J. J. Shepherd, G. Booth, A. Grüneis, and A. Alavi, "Full configuration interaction perspective on the homogeneous electron gas," *Phys. Rev. B* **85**, 081103 (2012).
- ³⁸C. Daday, S. Smart, G. H. Booth, A. Alavi, and C. Filippi, "Full Configuration Interaction Excitations of Ethene and Butadiene: Resolution of an Ancient Question," *J. Chem. Theory Comput.* **8**, 4441–4451 (2012).
- ³⁹E. Giner, A. Scemama, and M. Caffarel, "Using perturbatively selected configuration interaction in quantum Monte Carlo calculations," *Can. J. Chem.* **91**, 879–885 (2013).
- ⁴⁰F. A. Evangelista, "Adaptive multiconfigurational wave functions," *J. Chem. Phys.* **140**, 124114 (2014), arXiv:1403.4117v2.
- ⁴¹W. Liu and M. R. Hoffmann, "SDS: the 'static–dynamic–static' framework for strongly correlated electrons," *Theor. Chem. Acc.* **133**, 1481 (2014).
- ⁴²W. Liu and M. R. Hoffmann, "iCI: Iterative CI toward full CI," *J. Chem. Theory Comput.* **12**, 1169–1178 (2016).
- ⁴³R. E. Thomas, D. Opalka, C. Overy, P. J. Knowles, A. Alavi, and G. H. Booth, "Analytic nuclear forces and molecular properties from full configuration interaction quantum Monte Carlo," *J. Chem. Phys.* **143**, 054108 (2015), arXiv:1507.05503.
- ⁴⁴E. Giner, A. Scemama, and M. Caffarel, "Fixed-node diffusion monte carlo potential energy curve of the fluorine molecule F_2 using selected configuration interaction trial wavefunctions," *J. Chem. Phys.* **142**, 044115 (2015), arXiv:1408.3672.
- ⁴⁵N. S. Blunt, S. D. Smart, G. H. Booth, and A. Alavi, "An excited-state approach within full configuration interaction quantum Monte Carlo," *J. Chem. Phys.* **143**, 134117 (2015), arXiv:1508.04680.
- ⁴⁶N. S. Blunt, S. D. Smart, J. A. F. Kersten, J. S. Spencer, G. H. Booth, and A. Alavi, "Semi-stochastic full configuration interaction quantum Monte Carlo: Developments and application," *J. Chem. Phys.* **142**, 184107 (2015), arXiv:arXiv:1502.04847v1.
- ⁴⁷N. S. Blunt, "Communication: An efficient and accurate perturbative correction to initiator full configuration interaction quantum Monte Carlo," *J. Chem. Phys.* **148**, 221101 (2018), arXiv:1804.09528.
- ⁴⁸N. S. Blunt, "A hybrid approach to extending selected configuration interaction and full configuration interaction quantum Monte Carlo," *J. Chem. Phys.* **151**, 174103 (2019), arXiv:1908.04158.
- ⁴⁹N. S. Blunt, A. J. W. Thom, and C. J. C. Scott, "Preconditioning and Perturbative Estimators in Full Configuration Interaction Quantum Monte Carlo," *J. Chem. Theory Comput.* **15**, 3537–3551 (2019), arXiv:1901.06348.
- ⁵⁰N. Zhang, W. Liu, and M. R. Hoffmann, "Iterative Configuration Interaction with Selection," *J. Chem. Theory Comput.* , acs.jctc.9b01200 (2020), arXiv:1911.12506.
- ⁵¹O. Weser, K. Guther, K. Ghanem, and G. L. Manni, "Stochastic generalized active space self-consistent field: Theory and application," *J. Chem. Theory Comput.* **18**, 251–272 (2022).
- ⁵²O. Weser, A. Alavi, and G. L. Manni, "Exploiting locality in full configuration interaction Quantum Monte Carlo for fast excitation generation," *J. Chem. Theory Comput.* **19**, 9118–9135 (2023).
- ⁵³N. M. Tubman, J. Lee, T. Y. Takeshita, M. Head-Gordon, and K. B. Whaley, "A deterministic alternative to the full configuration interaction quantum Monte Carlo method," *J. Chem. Phys.* **145**, 044112 (2016), arXiv:1603.02686.
- ⁵⁴A. A. Holmes, N. M. Tubman, and C. J. Umrigar, "Heat-bath configuration interaction: An efficient selected configuration interaction algorithm inspired by heat-bath sampling," *J. Chem. Theory Comput.* **12**, 3674–3680 (2016).
- ⁵⁵J. Li, M. Otten, A. A. Holmes, S. Sharma, and C. J. Umrigar, "Fast semistochastic heat-bath configuration interaction," *J. Chem. Phys.* **149**, 214110 (2018).
- ⁵⁶N. M. Tubman, C. D. Freeman, D. S. Levine, D. Hait, M. Head-Gordon, and K. B. Whaley, "Modern Approaches to Exact Diagonalization and Selected Configuration Interaction with the Adaptive Sampling CI Method," *J. Chem. Theory Comput.* **16**, 2139–2159 (2020), arXiv:1807.00821.
- ⁵⁷D. B. Williams-Young, N. M. Tubman, C. Mejuto-Zaera, and W. A. de Jong, "A parallel, distributed memory implementation of the adaptive sampling configuration interaction method," *J. Chem. Phys.* **158**, 214109 (2023).
- ⁵⁸J. J. Eriksen, F. Lipparini, and J. Gauss, "Virtual Orbital Many-Body Expansions: A Possible Route towards the Full Configuration Interaction Limit," *J. Phys. Chem. Lett.* **8**, 4633–4639 (2017), arXiv:1708.02103.
- ⁵⁹P. M. Zimmerman, "Incremental full configuration interaction," *J. Chem. Phys.* **146**, 104102 (2017).
- ⁶⁰J. J. Eriksen and J. Gauss, "Incremental treatments of the full configuration interaction problem," *Wiley Interdiscip. Rev. Comput. Mol. Sci.* , e1525 (2021).
- ⁶¹S. R. White, "Density matrix formulation for quantum renormalization groups," *Phys. Rev. Lett.* **69**, 2863–2866 (1992).
- ⁶²S. R. White, "Density-matrix algorithms for quantum renormalization groups," *Phys. Rev. B* **48**, 10345–10356 (1993).
- ⁶³U. Schollwöck, "The density-matrix renormalization group," *Rev. Mod. Phys.* **77**, 259–315 (2005), arXiv:0409292 [cond-mat].
- ⁶⁴U. Schollwöck, "The density-matrix renormalization group in the age of matrix product states," *Ann. Physics* **326**, 96–192 (2011), arXiv:1008.3477.
- ⁶⁵G. K.-L. Chan and S. Sharma, "The density matrix renormalization group in quantum chemistry." *Annu. Rev. Phys. Chem.* **62**, 465–81 (2011).
- ⁶⁶A. Baiardi and M. Reiher, "The density matrix renormalization group in chemistry and molecular physics: Recent developments and new challenges," *J. Chem. Phys.* **152**, 040903 (2020), arXiv:1910.00137.
- ⁶⁷Y. Xu, Y. Cheng, Y. Song, and H. Ma, "New density matrix renormalization group approaches for strongly correlated systems coupled with large environments," *J. Chem. Theory Comput.* **19**, 4781–4795 (2023).
- ⁶⁸A. Menczer, M. van Damme, A. Rask, L. Huntington, J. Hammond, S. S. Xantheas, M. Ganahl, and Ö. Legeza, "Parallel implementation of the density matrix renormalization group method achieving a quarter petaFLOPS performance on a single DGX-H100 GPU node," *J. Chem. Theory Comput.* **20**, 8397–8404 (2024).
- ⁶⁹N. Nakatani and G. K.-L. Chan, "Efficient tree tensor network states (TTNS) for quantum chemistry: Generalizations of the density matrix renormalization group algorithm," *J. Chem. Phys.* **138**, 134113 (2013), arXiv:1302.2298.
- ⁷⁰B. O. Roos, P. R. Taylor, and P. E. M. Siegbahn, "A complete active space SCF method (CASSCF) using a density matrix formulated super-CI approach," *Chem. Phys.* **48**, 157–173 (1980).

- ⁷¹B. O. Roos, "The complete active space SCF method in a Fock-matrix-based super-CI formulation," *Int. J. Quantum Chem.* **18**, 175–189 (1980).
- ⁷²J. E. T. Smith, B. Mussard, A. A. Holmes, and S. Sharma, "Cheap and Near Exact CASSCF with Large Active Spaces," *J. Chem. Theory Comput.* **13**, 5468–5478 (2017), arXiv:1708.07544.
- ⁷³D. S. Levine, D. Hait, N. M. Tubman, S. Lehtola, K. B. Whaley, and M. Head-Gordon, "CASSCF with extremely large active spaces using the adaptive sampling configuration interaction method," *J. Chem. Theory Comput.* **16**, 2340–2354 (2020), arXiv:1912.08379.
- ⁷⁴Y. Guo, N. Zhang, Y. Lei, and W. Liu, "iCISCF: An iterative configuration interaction-based multiconfigurational self-consistent field theory for large active spaces," *J. Chem. Theory Comput.* **17**, 7545–7561 (2021).
- ⁷⁵D. Zgid and M. Nooijen, "The density matrix renormalization group self-consistent field method: Orbital optimization with the density matrix renormalization group method in the active space," *J. Chem. Phys.* **128**, 144116 (2008).
- ⁷⁶N. Nakatani and S. Guo, "Density matrix renormalization group (DMRG) method as a common tool for large active-space CASSCF/CASPT2 calculations," *J. Chem. Phys.* **146**, 094102 (2017).
- ⁷⁷Y. Cheng, Z. Xie, and H. Ma, "Post-density matrix renormalization group methods for describing dynamic electron correlation with large active spaces," *J. Phys. Chem. Lett.* **13**, 904–915 (2022).
- ⁷⁸R. P. Feynman, "Simulating physics with computers," *Int. J. Theor. Phys.* **21**, 467–488 (1982).
- ⁷⁹A. Aspuru-Guzik, A. D. Dutoi, P. J. Love, and M. Head-Gordon, "Simulated quantum computation of molecular energies," *Science* **309**, 1704–1707 (2005).
- ⁸⁰A. Peruzzo, J. McClean, P. Shadbolt, M.-H. Yung, X.-Q. Zhou, P. J. Love, A. Aspuru-Guzik, and J. L. O'Brien, "A variational eigenvalue solver on a photonic quantum processor," *Nat. Commun.* **5**, 4213 (2014), arXiv:1304.3061.
- ⁸¹J. R. McClean, J. Romero, R. Babbush, and A. Aspuru-Guzik, "The theory of variational hybrid quantum-classical algorithms," *New J. Phys.* **18**, 023023 (2016), arXiv:1509.04279.
- ⁸²J. Romero, R. Babbush, J. R. McClean, C. Hempel, P. J. Love, and A. Aspuru-Guzik, "Strategies for quantum computing molecular energies using the unitary coupled cluster ansatz," *Quantum Sci. Technol.* **4**, 014008 (2018).
- ⁸³D. A. Fedorov, B. Peng, N. Govind, and Y. Alexeev, "VQE method: a short survey and recent developments," *Materials Theory* **6**, 2 (2022).
- ⁸⁴M. Cerezo, A. Arrasmith, R. Babbush, S. C. Benjamin, S. Endo, K. Fujii, J. R. McClean, K. Mitarai, X. Yuan, L. Cincio, and P. J. Coles, "Variational quantum algorithms," *Nature Reviews Physics* **3**, 625–644 (2021).
- ⁸⁵J. Tilly, H. Chen, S. Cao, D. Picozzi, K. Setia, Y. Li, E. Grant, L. Wossnig, I. Rungger, G. H. Booth, and J. Tennyson, "The Variational Quantum Eigensolver: A review of methods and best practices," *Phys. Rep.* **986**, 1–128 (2022).
- ⁸⁶Y. Cao, J. Romero, J. P. Olson, M. Degroote, P. D. Johnson, M. Kieferová, I. D. Kivlichan, T. Menke, B. Peropadre, N. P. D. Sawaya, S. Sim, L. Veis, and A. Aspuru-Guzik, "Quantum Chemistry in the Age of Quantum Computing," *Chem. Rev.* **119**, 10856–10915 (2019), arXiv:1812.09976.
- ⁸⁷M. Motta and J. E. Rice, "Emerging quantum computing algorithms for quantum chemistry," *Wiley Interdiscip. Rev. Comput. Mol. Sci.* **12**, e1580 (2021).
- ⁸⁸A. Baiardi, M. Christandl, and M. Reiher, "Quantum computing for molecular biology," *ChemBioChem* **24**, e202300120 (2023).
- ⁸⁹W. J. Hunt, P. J. Hay, and W. A. Goddard III, "Self-consistent procedures for generalized valence bond wavefunctions. applications H₃, bh, H₂O, C₂H₆, and O₂," *J. Chem. Phys.* **57**, 738 (1972).
- ⁹⁰W. A. Goddard and L. B. Harding, "The Description of Chemical Bonding From Ab Initio Calculations," *Annu. Rev. Phys. Chem.* **29**, 363–396 (1978).
- ⁹¹D. W. Small and M. Head-Gordon, "Tractable spin-pure methods for bond breaking: Local many-electron spin-vector sets and an approximate valence bond model," *J. Chem. Phys.* **130**, 084103 (2009).
- ⁹²D. W. Small and M. Head-Gordon, "Post-modern valence bond theory for strongly correlated electron spins," *Phys. Chem. Chem. Phys.* **13**, 19285 (2011).
- ⁹³D. W. Small and M. Head-Gordon, "A fusion of the closed-shell coupled cluster singles and doubles method and valence-bond theory for bond breaking," *J. Chem. Phys.* **137**, 114103 (2012).
- ⁹⁴D. W. Small, K. V. Lawler, and M. Head-Gordon, "Coupled Cluster Valence Bond Method: Efficient Computer Implementation and Application to Multiple Bond Dissociations and Strong Correlations in the Acenes," *J. Chem. Theory Comput.* **10**, 2027–2040 (2014).
- ⁹⁵D. W. Small and M. Head-Gordon, "Coupled cluster valence bond theory for open-shell systems with application to very long range strong correlation in a polycarbene dimer," *J. Chem. Phys.* **147**, 024107 (2017).
- ⁹⁶D. W. Small and M. Head-Gordon, "Independent amplitude approximations in coupled cluster valence bond theory: Incorporation of 3-electron-pair correlation and application to spin frustration in the low-lying excited states of a ferredoxin-type tetrametallic iron-sulfur cluster," *J. Chem. Phys.* **149**, 144103 (2018).
- ⁹⁷J. Lee, D. W. Small, and M. Head-Gordon, "Open-shell coupled-cluster valence-bond theory augmented with an independent amplitude approximation for three-pair correlations: Application to a model oxygen-evolving complex and single molecular magnet," *J. Chem. Phys.* **149**, 244121 (2018).
- ⁹⁸J. Gerratt and M. Raimondi, "The Spin-Coupled Valence Bond Theory of Molecular Electronic Structure. I. Basic Theory and Application to the Formula States of BeH," *Proc. R. Soc. A Math. Phys. Eng. Sci.* **371**, 525–552 (1980).
- ⁹⁹D. L. Cooper, J. Gerratt, and M. Raimondi, "Spin-coupled valence bond theory," *Int. Rev. Phys. Chem.* **7**, 59–80 (1988).
- ¹⁰⁰P. R. Surján, "An Introduction to the Theory of Geminals," in *Correl. Localization*, Vol. 203 (Springer, Berlin, Heidelberg, 1999) pp. 63–88.
- ¹⁰¹V. A. Rassolov, "A geminal model chemistry," *J. Chem. Phys.* **117**, 5978–5987 (2002).
- ¹⁰²P. A. Johnson, P. W. Ayers, P. A. Limacher, S. D. Baerdemacker, D. V. Neck, and P. Bultinck, "A size-consistent approach to strongly correlated systems using a generalized antisymmetrized product of nonorthogonal geminals," *Comput. Theor. Chem.* **1003**, 101–113 (2013).
- ¹⁰³P. A. Limacher, P. W. Ayers, P. A. Johnson, S. De Baerdemacker, D. Van Neck, and P. Bultinck, "A New Mean-Field Method Suitable for Strongly Correlated Electrons: Computationally Facile Antisymmetric Products of Nonorthogonal Geminals," *J. Chem. Theory Comput.* **9**, 1394–1401 (2013).
- ¹⁰⁴P. Tecmer, K. Boguslawski, P. A. Johnson, P. A. Limacher, M. Chan, T. Verstraelen, and P. W. Ayers, "Assessing the Accuracy of New Geminal-Based Approaches," *J. Phys. Chem. A* **118**, 9058–9068 (2014).

- ¹⁰⁵E. Pastorczak and K. Pernal, “ERPA–APSG: a computationally efficient geminal-based method for accurate description of chemical systems,” *Phys. Chem. Chem. Phys.* **17**, 8622–8626 (2015).
- ¹⁰⁶H. R. Larsson, C. A. Jiménez-Hoyos, and G. K.-L. Chan, “Minimal matrix product states and generalizations of mean-field and geminal wave functions,” *J. Chem. Theory Comput.* **16**, 5057–5066 (2020), arXiv:2005.03703.
- ¹⁰⁷A. I. Krylov, C. D. Sherrill, E. F. C. Byrd, and M. Head-Gordon, “Size-consistent wave functions for nondynamical correlation energy: The valence active space optimized orbital coupled-cluster doubles model,” *J. Chem. Phys.* **109**, 10669 (1998).
- ¹⁰⁸P. Piecuch, S. A. Kucharski, and R. J. Bartlett, “Coupled-cluster methods with internal and semi-internal triply and quadruply excited clusters: CCSDt and CCSDtq approaches,” *J. Chem. Phys.* **110**, 6103 (1999).
- ¹⁰⁹J. Olsen, “The initial implementation and applications of a general active space coupled cluster method,” *J. Chem. Phys.* **113**, 7140 (2000).
- ¹¹⁰P. Piecuch, M. Wloch, J. R. Gour, and A. Kinal, “Single-reference, size-extensive, non-iterative coupled-cluster approaches to bond breaking and biradicals,” *Chem. Phys. Lett.* **418**, 467–474 (2006).
- ¹¹¹P. Piecuch, “Active-space coupled-cluster methods,” *Mol. Phys.* **108**, 2987–3015 (2010).
- ¹¹²J. Shen and P. Piecuch, “Combining active-space coupled-cluster methods with moment energy corrections via the CC(P ; Q) methodology, with benchmark calculations for biradical transition states,” *J. Chem. Phys.* **136**, 144104 (2012).
- ¹¹³J. Shen and P. Piecuch, “Merging active-space and renormalized coupled-cluster methods via the cc(p;q) formalism, with benchmark calculations for singlet–triplet gaps in biradical systems,” *J. Chem. Theory Comput.* **8**, 4968–4988 (2012).
- ¹¹⁴A. Köhn, M. Hanauer, L. A. Mück, T.-C. Jagau, and J. Gauss, “State-specific multireference coupled-cluster theory,” *Wiley Interdiscip. Rev.: Comput. Mol. Sci.* **3**, 176–197 (2013).
- ¹¹⁵I. Magoulas, J. Shen, and P. Piecuch, “Addressing strong correlation by approximate coupled-pair methods with active-space and full treatments of three-body clusters,” *Molecular Physics* (2022), 10.1080/00268976.2022.2057365.
- ¹¹⁶J. A. Parkhill, K. Lawler, and M. Head-Gordon, “The perfect quadruples model for electron correlation in a valence active space,” *J. Chem. Phys.* **130**, 084101 (2009).
- ¹¹⁷J. A. Parkhill and M. Head-Gordon, “A tractable and accurate electronic structure method for static correlations: the perfect hexuples model,” *J. Chem. Phys.* **133**, 024103 (2010).
- ¹¹⁸S. Lehtola, J. Parkhill, and M. Head-Gordon, “Cost-effective description of strong correlation: Efficient implementations of the perfect quadruples and perfect hexuples models,” *J. Chem. Phys.* **145**, 134110 (2016), arXiv:1609.00077.
- ¹¹⁹A. C. Hurley, J. Lennard-Jones, and J. A. Pople, “The Molecular Orbital Theory of Chemical Valency. XVI. A Theory of Paired-Electrons in Polyatomic Molecules,” *Proc. R. Soc. A Math. Phys. Eng. Sci.* **220**, 446–455 (1953).
- ¹²⁰I. I. Ukrainkii, “New variational function in the theory of quasi-one-dimensional metals,” *Theor. Math. Phys.* **32**, 816–822 (1977).
- ¹²¹J. Cullen, “Generalized valence bond solutions from a constrained coupled cluster method,” *Chem. Phys.* **202**, 217–229 (1996).
- ¹²²G. J. O. Beran, B. Austin, A. Sodt, and M. Head-Gordon, “Unrestricted perfect pairing: the simplest wave-function-based model chemistry beyond mean field,” *J. Phys. Chem. A* **109**, 9183–92 (2005).
- ¹²³S. Lehtola, J. Parkhill, and M. Head-Gordon, “Orbital optimisation in the perfect pairing hierarchy: applications to full-valence calculations on linear polyacenes,” *Mol. Phys.* **116**, 547–560 (2018), arXiv:1705.01678.
- ¹²⁴K. Nakayama, H. Nakano, and K. Hirao, “Theoretical study of the $\pi \rightarrow \pi^*$ excited states of linear polyenes: The energy gap between $1^1B_u^+$ and $2^1A_g^-$ states and their character,” *Int. J. Quantum Chem.* **66**, 157–175 (1998).
- ¹²⁵Y. Kurashige, H. Nakano, Y. Nakao, and K. Hirao, “The $\pi \rightarrow \pi^*$ excited states of long linear polyenes studied by the CASCI-MRMP method,” *Chem. Phys. Lett.* **400**, 425–429 (2004).
- ¹²⁶T. Bally, D. A. Hrovat, and W. Thatcher Borden, “Attempts to model neutral solitons in polyacetylene by ab initio and density functional methods. The nature of the spin distribution in polyenyl radicals,” *Phys. Chem. Chem. Phys.* **2**, 3363–3371 (2000).
- ¹²⁷J. Hachmann, W. Cardoen, and G. K.-L. Chan, “Multireference correlation in long molecules with the quadratic scaling density matrix renormalization group,” *J. Chem. Phys.* **125**, 144101 (2006), arXiv:0606115 [cond-mat].
- ¹²⁸W. Hu and G. K.-L. Chan, “Excited-State Geometry Optimization with the Density Matrix Renormalization Group, as Applied to Polyenes,” *J. Chem. Theory Comput.* **11**, 3000–3009 (2015), arXiv:1502.07731.
- ¹²⁹P. B. Karadakov, J. Gerratt, G. Raos, D. L. Cooper, and M. Raimondi, “Spin-coupled study of the electronic structure of polyenyl radicals $C_3H_5-C_9H_{11}$,” *J. Am. Chem. Soc.* **116**, 2075–2084 (1994).
- ¹³⁰Y. Luo, L. Song, W. Wu, D. Danovich, and S. Shaik, “The ground and excited states of polyenyl radicals $C_{2n-1}H_{2n+1}$ ($n = 2-13$): A valence bond study,” *ChemPhysChem* **5**, 515–528 (2004).
- ¹³¹J. Gu, Y. Lin, B. Ma, W. Wu, and S. Shaik, “Covalent excited states of polyenes $C_{2n}H_{2n+2}$ ($n = 2-8$) and polyenyl radicals $C_{2n-1}H_{2n+1}$ ($n = 2-8$): An ab initio valence bond study,” *J. Chem. Theory Comput.* **4**, 2101–2107 (2008).
- ¹³²J. H. Starcke, M. Wormit, and A. Dreuw, “Nature of the lowest excited states of neutral polyenyl radicals and polyene radical cations,” *J. Chem. Phys.* **131**, 144311 (2009).
- ¹³³W. Kurlancheek, R. Lochan, K. Lawler, and M. Head-Gordon, “Exploring the competition between localization and delocalization of the neutral soliton defect in polyenyl chains with the orbital optimized second order opposite spin method,” *J. Chem. Phys.* **136**, 054113 (2012).
- ¹³⁴J. B. Schriber and F. A. Evangelista, “Adaptive Configuration Interaction for Computing Challenging Electronic Excited States with Tunable Accuracy,” *J. Chem. Theory Comput.* **13**, 5354–5366 (2017).
- ¹³⁵A. Köhn and J. Olsen, “Orbital-optimized coupled-cluster theory does not reproduce the full configuration-interaction limit,” *J. Chem. Phys.* **122**, 084116 (2005).
- ¹³⁶J. A. Parkhill and M. Head-Gordon, “A sparse framework for the derivation and implementation of fermion algebra,” *Mol. Phys.* **108**, 513–522 (2010).
- ¹³⁷J. Catalán and J. L. G. de Paz, “On the ordering of the first two excited electronic states in all-trans linear polyenes,” *J. Chem. Phys.* **120**, 1864 (2004).
- ¹³⁸J. Lehtola, M. Hakala, A. Sakko, and K. Hämmäläinen, “ERKALE – a flexible program package for x-ray properties of atoms and molecules,” *J. Comput. Chem.* **33**, 1572–1585 (2012).
- ¹³⁹S. Lehtola, “ERKALE – HF/DFT from Hel,” (2023), accessed 23 March 2023.
- ¹⁴⁰T. Van Voorhis and M. Head-Gordon, “A geometric approach to direct minimization,” *Mol. Phys.* **100**, 1713–1721 (2002).
- ¹⁴¹T. Van Voorhis and M. Head-Gordon, “Implementation of generalized valence bond-inspired coupled cluster theories,” *J. Chem. Phys.* **117**, 9190–9201 (2002).

- ¹⁴²B. D. Dunietz, T. Van Voorhis, and M. Head-Gordon, "Geometric direct minimization of Hartree-Fock calculations involving open shell wavefunctions with spin restricted orbitals," *J. Theor. Comput. Chem.* **1**, 255–261 (2002).
- ¹⁴³J. Nocedal and S. Wright, *Numerical Optimization*, Springer Series in Operations Research and Financial Engineering (Springer New York, New York, 1999).
- ¹⁴⁴T. H. Dunning, "Gaussian basis sets for use in correlated molecular calculations. I. The atoms boron through neon and hydrogen," *J. Chem. Phys.* **90**, 1007 (1989).
- ¹⁴⁵S. Lehtola and H. Jónsson, "Unitary optimization of localized molecular orbitals," *J. Chem. Theory Comput.* **9**, 5365–5372 (2013).
- ¹⁴⁶S. Lehtola and H. Jónsson, "Pipek-Mezey orbital localization using various partial charge estimates," *J. Chem. Theory Comput.* **10**, 642–649 (2014).
- ¹⁴⁷T. Sano, "Elementary Jacobi rotation method for generalized valence bond perfect-pairing calculations combined with simple procedure for generating reliable initial orbitals," *J. Mol. Struct. THEOCHEM* **528**, 177–191 (2000).
- ¹⁴⁸N. H. F. Beebe and J. Linderberg, "Simplifications in the Two-Electron Integral Array in Molecular Calculations," *Int. J. Quant. Chem.* **12**, 683–705 (1977).
- ¹⁴⁹T. B. Pedersen, S. Lehtola, I. F. Galván, and R. Lindh, "The versatility of the Cholesky decomposition in electronic structure theory," *Wiley Interdiscip. Rev. Comput. Mol. Sci.* **14**, e1692 (2023).
- ¹⁵⁰H. Koch, A. Sánchez de Merás, and T. B. Pedersen, "Reduced scaling in electronic structure calculations using Cholesky decompositions," *J. Chem. Phys.* **118**, 9481–9484 (2003).
- ¹⁵¹W. M. Flicker, O. A. Mosher, and A. Kuppermann, "Singlet \rightarrow triplet transitions in methyl-substituted ethylenes," *Chem. Phys. Lett.* **36**, 56–60 (1975).
- ¹⁵²E. H. Van Veen, "Low-energy electron-impact spectroscopy on ethylene," *Chem. Phys. Lett.* **41**, 540–543 (1976).
- ¹⁵³O. A. Mosher, W. M. Flicker, and A. Kuppermann, "Triplet states in 1,3-butadiene," *Chem. Phys. Lett.* **19**, 332–333 (1973).
- ¹⁵⁴O. A. Mosher, W. M. Flicker, and A. Kuppermann, "Electronic spectroscopy of s-trans 1,3-butadiene by electron impact," *J. Chem. Phys.* **59**, 6502–6511 (1973).
- ¹⁵⁵N. G. Minnaard and E. Havinga, "Some aspects of the electronic spectra of 1,3-cyclohexadiene, (E)- and (Z)-1,3,5-hexatriene," *Recl. des Trav. Chim. des Pays-Bas* **92**, 1179–1188 (1973).
- ¹⁵⁶W. M. Flicker, O. A. Mosher, and A. Kuppermann, "Low energy, variable angle electron-impact excitation of 1,3,5-hexatriene," *Chem. Phys. Lett.* **45**, 492–497 (1977).
- ¹⁵⁷A. Kuppermann, W. M. Flicker, and O. A. Mosher, "Electronic spectroscopy of polyatomic molecules by low-energy, variable-angle electron impact," *Chem. Rev.* **79**, 77–90 (1979).
- ¹⁵⁸M. Allan, L. Neuhaus, and E. Haselbach, "(all-E)-1,3,5,7-Octatetraene: Electron-Energy-Loss and Electron-Transmission Spectra," *Helv. Chim. Acta* **67**, 1776–1782 (1984).
- ¹⁵⁹D. Hait and M. Head-Gordon, "Delocalization Errors in Density Functional Theory Are Essentially Quadratic in Fractional Occupation Number," *J. Phys. Chem. Lett.* **9**, 6280–6288 (2018).
- ¹⁶⁰P. Plessis and P. Marmet, "Electroionization study of ethylene: ionization and appearance energies, ion-pair formations, and negative ions," *Can. J. Phys.* **65**, 165–172 (1987).
- ¹⁶¹B. A. Williams and T. A. Cool, "Two-photon spectroscopy of Rydberg states of jet-cooled C_2H_4 and C_2D_4 ," *J. Chem. Phys.* **94**, 6358–6366 (1991).
- ¹⁶²K. Ohno, K. Okamura, H. Yamakado, S. Hoshino, T. Takami, and M. Yamauchi, "Penning ionization of HCHO, CH_2CH_2 , and CH_2CHCHO by collision with $he^*(2^3s)$ metastable atoms," *J. Phys. Chem.* **99**, 14247–14253 (1995).
- ¹⁶³W. G. Mallard, J. H. Miller, and K. C. Smyth, "The *ns* Rydberg series of 1,3-*trans*-butadiene observed using multiphoton ionization," *J. Chem. Phys.* **79**, 5900–5905 (1983).
- ¹⁶⁴G. Bieri, F. Burger, E. Heilbronner, and J. P. Maier, "Valence Ionization Energies of Hydrocarbons," *Helv. Chim. Acta* **60**, 2213–2233 (1977).
- ¹⁶⁵M. Allan, J. Dannacher, and J. P. Maier, "Radiative and fragmentation decay of the cations of *trans*- and *cis*-1,3,5-hexatriene and of all *trans*-1,3,5-heptatriene in the $\tilde{A}(\pi^{-1})$ states, studied by emission and photoelectron-photoion coincidence spectroscopy," *J. Chem. Phys.* **73**, 3114–3122 (1980).
- ¹⁶⁶T. B. Jones and J. P. Maier, "Study of the radical cation of all *trans*-1,3,5,7-octatetraene by its emission, $\tilde{A}^2A_u \rightarrow \tilde{X}^2B_g$, and by photoelectron spectroscopy," *Int. J. Mass Spectrom. Ion Phys.* **31**, 287–291 (1979).
- ¹⁶⁷J. Bois and T. Körzdörfer, "Size-dependence of nonempirically tuned DFT starting points for G_0W_0 applied to π -conjugated molecular chains," *J. Chem. Theory Comput.* **13**, 4962–4971 (2017), arXiv:1706.00196.
- ¹⁶⁸F. Aquilante, K. P. Jensen, and B. O. Roos, "The allyl radical revisited: a theoretical study of the electronic spectrum," *Chem. Phys. Lett.* **380**, 689–698 (2003).
- ¹⁶⁹I. Fischer and P. Chen, "Allyl-A Model System for the Chemical Dynamics of Radicals," *J. Phys. Chem. A* **106**, 4291–4300 (2002).
- ¹⁷⁰D. Griller and F. P. Lossing, "Thermochemistry of α -aminoalkyl radicals," *J. Am. Chem. Soc.* **103**, 1586–1587 (1981).
- ¹⁷¹F. A. Houle and J. L. Beauchamp, "Detection and investigation of allyl and benzyl radicals by photoelectron spectroscopy," *J. Am. Chem. Soc.* **100**, 3290–3294 (1978).
- ¹⁷²F. P. Lossing and J. C. Traeger, "Free radicals by mass spectrometry XLVI. heats of formation of C_5H_7 and C_5H_9 radicals and cations," *Int. J. Mass Spectrom. Ion Phys.* **19**, 9–22 (1976).
- ¹⁷³S. Pignataro, A. Cassuto, and F. P. Lossing, "Free radicals by mass spectrometry. XXXVI. Ionization potentials of conjugated and nonconjugated radicals," *J. Am. Chem. Soc.* **89**, 3693–3697 (1967).
- ¹⁷⁴M. Haranczyk and M. Gutowski, "Visualization of molecular orbitals and the related electron densities," *J. Chem. Theory Comput.* **4**, 689–693 (2008).
- ¹⁷⁵E. Epifanovsky, A. T. B. Gilbert, X. Feng, J. Lee, Y. Mao, N. Mardirossian, P. Pokhilko, A. F. White, M. P. Coons, A. L. Dempwolff, Z. Gan, D. Hait, P. R. Horn, L. D. Jacobson, I. Kaliman, J. Kusmann, A. W. Lange, K. U. Lao, D. S. Levine, J. Liu, S. C. McKenzie, A. F. Morrison, K. D. Nanda, F. Plasser, D. R. Rehn, M. L. Vidal, Z.-Q. You, Y. Zhu, B. Alam, B. J. Albrecht, A. Aldossary, E. Alguire, J. H. Andersen, V. Athavale, D. Barton, K. Begam, A. Behn, N. Bellonzi, Y. A. Bernard, E. J. Berquist, H. G. A. Burton, A. Carreras, K. Carter-Fenk, R. Chakraborty, A. D. Chien, K. D. Closser, V. Cofer-Shabica, S. Dasgupta, M. de Wergifosse, J. Deng, M. Diedenhofen, H. Do, S. Ehlert, P.-T. Fang, S. Fatehi, Q. Feng, T. Friedhoff, J. Gayvert, Q. Ge, G. Gidofalvi, M. Goldey, J. Gomes, C. E. González-Espinoza, S. Gulania, A. O. Gunina, M. W. D. Hanson-Heine, P. H. P. Harbach, A. Hauser, M. F. Herbst, M. Hernández Vera, M. Hodecker, Z. C. Holden, S. Houck, X. Huang, K. Hui, B. C. Huynh, M. Ivanov, Á. Jász, H. Ji, H. Jiang, B. Kaduk,

- S. Kähler, K. Khistyayev, J. Kim, G. Kis, P. Klunzinger, Z. Koczor-Benda, J. H. Koh, D. Kosenkov, L. Koulias, T. Kowalczyk, C. M. Krauter, K. Kue, A. Kunitsa, T. Kus, I. Ladjánszki, A. Landau, K. V. Lawler, D. Lefrancois, S. Lehtola, R. R. Li, Y.-P. Li, J. Liang, M. Liebenthal, H.-H. Lin, Y.-S. Lin, F. Liu, K.-Y. Liu, M. Loipersberger, A. Luenser, A. Manjanath, P. Manohar, E. Mansoor, S. F. Manzer, S.-P. Mao, A. V. Marenich, T. Markovich, S. Mason, S. A. Maurer, P. F. McLaughlin, M. F. S. J. Menger, J.-M. Mewes, S. A. Mewes, P. Morgante, J. W. Mullinax, K. J. Oosterbaan, G. Paran, A. C. Paul, S. K. Paul, F. Pavošević, Z. Pei, S. Prager, E. I. Proynov, Á. Rák, E. Ramos-Cordoba, B. Rana, A. E. Rask, A. Rettig, R. M. Richard, F. Rob, E. Rossomme, T. Scheele, M. Scheurer, M. Schneider, N. Sergueev, S. M. Sharada, W. Skomorowski, D. W. Small, C. J. Stein, Y.-C. Su, E. J. Sundstrom, Z. Tao, J. Thirman, G. J. Tornai, T. Tsuchimochi, N. M. Tubman, S. P. Veccham, O. Vydrov, J. Wenzel, J. Witte, A. Yamada, K. Yao, S. Yeganeh, S. R. Yost, A. Zech, I. Y. Zhang, X. Zhang, Y. Zhang, D. Zuev, A. Aspuru-Guzik, A. T. Bell, N. A. Besley, K. B. Bravaya, B. R. Brooks, D. Casanova, J.-D. Chai, S. Coriani, C. J. Cramer, G. Cserey, A. E. DePrince, R. A. DiStasio, A. Dreuw, B. D. Dunietz, T. R. Furlani, W. A. Goddard, S. Hammes-Schiffer, T. Head-Gordon, W. J. Hehre, C.-P. Hsu, T.-C. Jagau, Y. Jung, A. Klamt, J. Kong, D. S. Lambrecht, W. Liang, N. J. Mayhall, C. W. McCurdy, J. B. Neaton, C. Ochsenfeld, J. A. Parkhill, R. Peverati, V. A. Rassolov, Y. Shao, L. V. Slipchenko, T. Stauch, R. P. Steele, J. E. Subotnik, A. J. W. Thom, A. Tkatchenko, D. G. Truhlar, T. Van Voorhis, T. A. Wesolowski, K. B. Whaley, H. L. Woodcock, P. M. Zimmerman, S. Faraji, P. M. W. Gill, M. Head-Gordon, J. M. Herbert, and A. I. Krylov, “Software for the frontiers of quantum chemistry: An overview of developments in the Q-Chem 5 package,” *J. Chem. Phys.* **155**, 084801 (2021).
- ¹⁷⁶S. Lehtola, N. M. Tubman, K. B. Whaley, and M. Head-Gordon, “Cluster decomposition of full configuration interaction wave functions: A tool for chemical interpretation of systems with strong correlation,” *J. Chem. Phys.* **147**, 154105 (2017), arXiv:1707.04376.
- ¹⁷⁷R. H. Myhre, “Demonstrating that the nonorthogonal orbital optimized coupled cluster model converges to full configuration interaction,” *J. Chem. Phys.* **148**, 094110 (2018).